Communication

Quantitative MRI Assessment of Post-surgical Spinal Cord Injury Through Radiomic Analysis

Azadeh Sharafi *, Andrew P Klein, Kevin M Koch

Posted Date: 4 November 2024

doi: 10.20944/preprints202411.0118.v1

Keywords: Radiomics; Spinal cord Injury; Multi-Spectral Imaging; Magnetic Resonance Imaging; Metal artefact

 doi:10.20944/preprints202411.0118.v1

Communication

Quantitative MRI Assessment of Post-surgical Spinal Cord Injury Through Radiomic Analysis

Azadeh Sharafi *, Andrew Klein and Kevin Koch

Radiology Department, Medical College of Wisconsin, WI, 53226, USA
* Correspondence: asharafi@mcw.edu

Abstract: Purpose: This study investigates radiomics efficacy in post-surgical traumatic spinal cord injury (SCI), overcoming MRI limitations from metal artifacts to enhance diagnosis, severity assessment, and lesion characterization for prognosis and therapy guidance. **Background**: Traumatic spinal cord injury (SCI) causes severe neurological deficits. While MRI allows qualitative injury evaluation, standard imaging alone has limitations for precise SCI diagnosis, severity stratification, and pathology characterization needed to guide prognosis and therapy. Radiomics enables quantitative tissue phenotyping by extracting a high-dimensional set of descriptive texture features from medical images. However, the efficacy of postoperative radiomic quantification in the presence of metal-induced MRI artifacts from spinal instrumentation has yet to be fully explored. **Methods**: 50 healthy controls and 12 SCI patients post-stabilization surgery underwent 3D multi-spectral MRI. Automated spinal cord segmentation was followed by radiomic feature extraction. Supervised machine learning categorized SCI versus controls, injury severity, and lesion location relative to instrumentation. **Results:** Radiomics differentiated SCI patients (Matthews correlation coefficient (MCC) 0.97; accuracy 1.0), categorized injury severity (MCC: 0.95; ACC: 0.98) and localized lesions (MCC: 0.85; ACC: 0.90). Combined T_1 and T_2 features outperformed individual modalities across tasks with gradient boosting models showing highest efficacy**. Conclusion:** The radiomic framework achieved excellent performance, differentiating SCI from controls and accurately categorizing injury severity. The ability to reliably quantify SCI severity and localization could potentially inform diagnosis, prognosis, and guide therapy. Further research is warranted to validate radiomic SCI biomarkers and explore clinical integration.

Keywords: Radiomics; Spinal cord Injury; Multi-Spectral Imaging; Magnetic Resonance Imaging; Metal artefact

1. Introduction

Traumatic spinal cord injury (SCI) is a devastating condition affecting millions of individuals worldwide. SCI profoundly impacts physical, psychological, and socioeconomic well-being [1]. In the United States alone, approximately 17,800 new SCI cases occur annually [2]. SCI can damage axons, neurons, glia, and blood vessels, resulting in temporary or permanent sensory and motor deficits below the lesion level [3]. Most SCIs occur at cervical levels, with common causes being motor vehicle collisions, falls, violence, and sports activities [2].

Magnetic resonance imaging (MRI) is the preferred modality for visualizing the spinal cord and soft tissues [4]. Conventional MRI protocols enable cord compression, signal changes, edema, hemorrhage, and morphologic alterations to be detected after injury. However, qualitative image evaluation has limitations in providing microstructural and functional details needed to guide SCI prognosis and management [5].

Quantitative MRI techniques like diffusion tensor imaging, magnetization transfer, and functional MRI have demonstrated potential for extracting precise biomarkers of post-traumatic cord integrity and function [6]. Still, these methods probe specific physiological phenomena in isolation. Radiomics offers a more holistic approach by extracting multiple descriptive features from medical

 doi:10.20944/preprints202411.0118.v1

images through high-throughput data characterization [7]. Radiomic methods have shown promise for prognosis in oncology [8]. Recently, radiomic techniques have been explored in spinal cord studies. Okimatsu et al. developed a radiomic model using T_2^*-weighted MRI and machine learning to predict neurological outcomes after acute cervical SCI [9]. However, a key challenge is that SCI frequently requires surgical stabilization involving the implantation of metallic instrumentation. The hardware can produce artifacts on conventional postoperative MRI [10] that disrupt quantitative radiomic analyses.

This study aimed to implement a radiomic modeling approach to analyze MRI of the instrumented spinal cord in SCI subjects. Multi-spectral imaging sequences were leveraged to suppress metal artifacts and thus enable unobstructed radiomic feature extraction at instrumented levels [11]. We hypothesized that radiomic signatures could reliably categorize SCI severity and lesion location. Successfully quantifying MRI traits in instrumented cords could ultimately enable monitoring of traumatic changes to inform SCI diagnosis and therapeutic regimens.

2. Materials and Methods

Reporting and analysis in this study followed the CheckList for EvaluAtion of Radiomics Research (CLEAR) documentation standard focusing on repeatability, reproducibility, and transparency of radiomic studies [12].

2.1. Study Cohorts

This study involved 12 subjects with traumatic SCI who underwent MRI scans 1-14 months (mean 7.08 ± 4.03) following surgical stabilization at cervical levels using metallic instrumentation. SCI severity was graded using the American Spinal Injury Association (ASIA) Impairment Scale (AIS). The study also included 50 healthy controls with no SCI or cord disorders history. Informed consent was obtained from all participants per our Institutional Review Board protocol. Table 1 summarizes the cohort demographics.

Table 1. Characteristics of the study cohorts.

Cohorts	Gender	Count	Age	BMI	ASIA: A	ASIA: B	ASIA: C	ASIA: D
Healthy	Female	25	47.52 ± 15.23	27.22 ± 7.18	0	0	0	0
	Male	26	48.50 ± 16.92	27.84 ± 4.67	0	0	0	0
	Total	51	48.02 ± 15.96	27.54 ± 5.98	0	0	0	0
SCI	Female	6	59.50 ± 18.62	25.57 ± 5.90	0	1	2	3
	Male	6	48.50 ± 21.95	23.52 ± 2.68	2	1	1	2
	Total	12	54.00 ± 20.24	24.54 ± 4.50	2	2	3	5

Imaging was performed at 3T (GE Signa Premier) using a 21-channel neurovascular coil. Multi-spectral 3D fast spin echo MRI was acquired to suppress metal artifacts [11]. Isotropic 1.2 mm resolution T_1 and T_2-weighted volumes were obtained with 8 spectral bins. Imaging parameters were TR/TE: T_1 - 750/8 ms, T_2 - 2100/60 ms, ARC 2x2 acceleration.

2.2. Image Analysis

The spinal cord was automatically segmented on T_1 and T_2 volumes using the Spinal Cord Toolbox deep learning model [13], followed by refinements to handle residual artifacts (Figure 1) [14]. Radiomic feature extraction was performed within cord segmentation using PyRadiomics [15]. A total of 1374 features describing intensity, shape, and texture patterns were generated from original and filtered images, including (wavelet, square, square root, logarithm, exponential, gradient, and local binary pattern).

 doi:10.20944/preprints202411.0118.v1

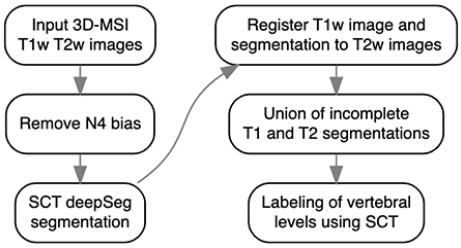

Figure 1. The flowchart depicts the processing pipeline for segmenting the spinal cord as suggested in [14]. First, N4 bias field correction is applied to the images to remove shading. Then, the SCT deep learning model segments the spinal cord individually on T_1 and T_2 volumes. However, these segmentations exhibit intermittent failures caused by metal implant artifacts. To mitigate these failures, the T_1 data is registered to the T_2 space. Then, a radial basis function algorithm integrates the T_1 and T_2 segmentations, thereby correcting the intermittent failures. Finally, the improved segmentation is used by SCT to label the vertebral levels automatically.

2.3. Classification Framework

The radiomic feature sets were input into a supervised machine-learning pipeline to differentiate SCI subjects from controls and categorize injury severity and cord location relative to the injury site. The dataset was divided into training (70%), validation (15%), and testing (15%) subsets. An automated modeling framework (H2O AutoML) evaluated various classifiers (random forest, XGBoost, neural networks, etc.) using 5-fold cross-validation on the training data [16]. The best model for each target was selected, and performance was assessed on the independent test set.

Three classification tasks were: 1) Differentiating SCI cases from healthy controls, 2) SCI severity (severe AIS A-B vs. non-severe AIS C-D), and 3) Lesion zone (above, at, or below instrumentation level). For each target, models were trained using T_1, T_2, or combined T_1+T_2 radiomic features to compare performance. Evaluation metrics were accuracy, Matthew's correlation coefficient (MCC), F1-score, and the area under the ROC (receiver operating characteristic) curve (AUC).

3. Results

Figure 2 depicts sample T_1 and T_2 weighted MRI images and the segmented cord on an instrumented slice.

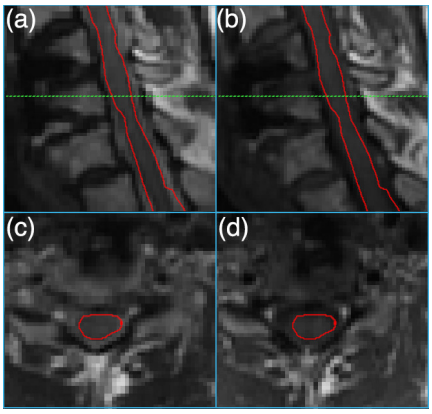

Figure 2. Sagittal **(a)** T_2-weighted and **(b)** T_1-weighted 3D-MSI MRI images of an instrumented damaged spinal cord. Axial sections, reformatted at the level of the dashed green line from (a) and (b), are shown in **(c)** and **(d)** respectively. The spinal cord is outlined in red in all images.

As shown in Figure 3, a combined T_1 and T_2 feature set achieved strong performance in discriminating between healthy controls and SCI patients, with 0.97 MCC, 0.98 F1 score, 1.00 Accuracy, and 1.00 AUC. For predicting injury severity, the T_1+T_2 model again achieved robust performance with 0.95 MCC, 0.98 F1 score, 0.98 Accuracy, and 0.99 AUC. The T_2 model achieved 0.86

 doi:10.20944/preprints202411.0118.v1

MCC and 0.94 Accuracy. For lesion zone classification, the T_1+T_2 model performed best with 0.85 MCC, 0.90 F1 score, 0.90 Accuracy, and 0.98 AUC. The T_2 model achieved 0.81 MCC and 0.88 Accuracy.

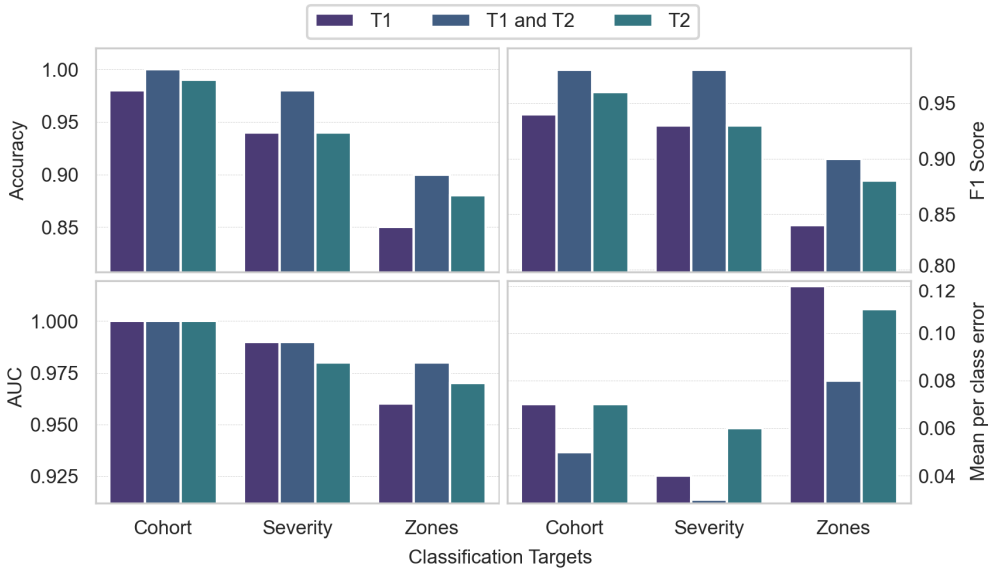

Figure 3. Comparison of accuracy, F1 score, area under the curve (AUC-ROC), and mean per-class error across radiomic classification tasks using T_1, T_2, and combined T_1/T_2 feature sets. The tasks include categorizing cohorts into healthy or spinal cord injury (SCI) groups, determining injury severity levels, and distinguishing between cord zones relative to the injury site.

Gradient boosting machine (GBM) models achieved the top performance for most tasks. The only exception was the zone classification task using T_1 features, for which XGBoost was optimal.

Overall, the combined T_1+T_2 models outperformed individual modalities across tasks. The models demonstrated excellent discrimination for SCI vs. controls and good predictive performance for injury severity. Results were strong but comparatively lower for the more challenging 3-class zone classification task.

4. Discussion

This study demonstrates the potential of a radiomic modeling approach for instrumented spinal cord MRI analysis in traumatic SCI. A key advance was the use of multi-spectral imaging to suppress instrumentation artifacts that can distort quantitative feature extraction. Radiomic SCI characterization could offer advantages over qualitative evaluation alone or standard diffusion/functional MRI methods that assess specific microstructural or physiological properties in isolation. The high-throughput radiomic feature set provides a more comprehensive phenotypic profiling of overall cord tissue traits linked to injury.

The radiomic framework reliably differentiated severe and non-severe SCI categories, achieving robust classification performance. This ability to determine injury severity, which has significant implications for prognosis and therapy, demonstrates clinical utility.

While global accuracy metrics were relatively high across tasks, lower MCC and F1 scores imply some degree of inter-class imbalance likely exists in the dataset. This imbalance means majority classes were more successfully predicted than minority classes. Techniques such as oversampling of minority classes or cost-sensitive learning could address this and improve MCC and F1 metrics. Additionally, discrimination power was weaker for more nuanced tasks like severity level or subtle zone differences. These findings warrant focused efforts on feature engineering and model tuning targeting MCC and F1 improvements.

When assessing the advantages of combined T_1 and T_2 features versus prolonged scan times, the MCC is particularly informative in the presence of class imbalance. For cohort differentiation, the

 doi:10.20944/preprints202411.0118.v1

MCC increase from 0.92 to 0.97 with combined features is substantial. However, the 0.92 baseline already indicates robust predictive power. In efficiency-focused clinical settings, marginal T_1+T_2 benefits may not outweigh longer scans, especially for resource optimization.

For severity classification, the MCC rose slightly from 0.86 to 0.95 with combined features. While showing an increase, the 0.86 T_2 baseline is respectable. The slight absolute MCC increase may have limited utility depending on clinical use. T_2 could suffice when efficiency is critical and acceptable severity discrimination is achievable. However, for applications where severity subtleties carry high stakes, the T_1+T_2 approach may provide value despite a longer scan time.

For multiclass zone classification, the more substantial MCC boost from 0.81 to 0.85 with T_1+T_2 features could justify extra scan time. While context-dependent, this degree of performance lift may warrant dual-acquisition protocols.

In summary, T_1+T_2 improved performance metrics across tasks. However, clinical value versus efficiency tradeoffs depends on the classification specifics and performance requirements.

Further feature engineering or integrating other imaging modalities could refine model performance. More extensive longitudinal studies are essential to fully explore clinical utility. Overall, radiomic modeling shows promise for quantitative SCI MRI, potentially guiding diagnosis and management.

Author Contributions: A.A and K.K; Data curation, A.A; Formal analysis, A.A; Funding acquisition, K.K; Investigation, K.K; Methodology, A.A; Project administration, K.K; Resources, K.K; Software, A.A; Supervision, K.K; Validation, A.A and K.K; Visualization, A.A; Writing – original draft, A.A; Writing – review & editing, A.K and K.K; All authors have read and agreed to the published version of the manuscript.

Funding: This research was funded by Department of Defense Congressionally Directed Medical Research Program, Spinal Cord Injury Research Program, award number W81XWH1910273.

Institutional Review Board Statement: The study was conducted in accordance with the Declaration of Helsinki and approved by the Institutional Review Board of Medical College of Wisconsin (protocol code *PRO00034880*, date of approval: 2/15/2024).

Informed Consent Statement: Informed consent was obtained from all subjects involved in the study.

Data Availability Statement: The data presented in this study are openly available in Mendeley Data at https://data.mendeley.com/datasets/sjpx7md7cf/1.

Conflicts of Interest: The authors declare no conflicts of interest. The funders had no role in the design of the study; in the collection, analyses, or interpretation of data; in the writing of the manuscript; or in the decision to publish the results.

References

1. Lee B, Cripps RA, Fitzharris M, Wing P (2014) The global map for traumatic spinal cord injury epidemiology: Update 2011, global incidence rate. Spinal cord 52:110–116
2. Singh A, Tetreault L, Kalsi-Ryan S, et al. (2014) Global prevalence and incidence of traumatic spinal cord injury. Clinical epidemiology 309–331
3. Dulin JN, Adler AF, Kumamaru H, et al. (2018) Injured adult motor and sensory axons regenerate into appropriate organotypic domains of neural progenitor grafts. Nature communications 9:84
4. Shabani S, Meyer BP, Budde MD, Wang MC (2021) Diagnostic imaging in spinal cord injury. Neurosurgery Clinics 32:323–331
5. Martin AR, Aleksanderek I, Cohen-Adad J, et al. (2016) Translating state-of-the-art spinal cord MRI techniques to clinical use: A systematic review of clinical studies utilizing DTI, MT, MWF, MRS, and fMRI. NeuroImage: Clinical 10:192–238
6. Cohen-Adad J, El Mendili M, Lehéricy S, et al. (2011) Demyelination and degeneration in the injured human spinal cord detected with diffusion and magnetization transfer MRI. Neuroimage 55:1024–1033
7. Lambin P, Leijenaar RT, Deist TM, et al. (2017) Radiomics: The bridge between medical imaging and personalized medicine. Nature reviews Clinical oncology 14:749–762
8. Aerts HJ, Velazquez ER, Leijenaar RT, et al. (2014) Decoding tumour phenotype by noninvasive imaging using a quantitative radiomics approach. Nature communications 5:4006
9. Okimatsu S, Maki S, Furuya T, et al. (2022) Determining the short-term neurological prognosis for acute cervical spinal cord injury using machine learning. Journal of Clinical Neuroscience 96:74–79.

 doi:10.20944/preprints202411.0118.v1

10. Hargreaves B, Worters PW, Pauly KB, et al. (2011) Metal induced artifacts in MRI. AJR American journal of roentgenology 197:547
11. Koch KM, Lorbiecki JE, Hinks RS, King KF (2009) A multispectral three-dimensional acquisition technique for imaging near metal implants. Magnetic Resonance in Medicine: An Official Journal of the International Society for Magnetic Resonance in Medicine 61:381–390
12. Kocak B, Baessler B, Bakas S, et al. (2023) CheckList for EvaluAtion of radiomics research (CLEAR): A step-by-step reporting guideline for authors and reviewers endorsed by ESR and EuSoMII. Insights into Imaging 14:75. https://doi.org/10.1186/s13244-023-01415-8
13. De Leener B, Lévy S, Dupont SM, et al. (2017) SCT: Spinal cord toolbox, an open-source software for processing spinal cord MRI data. Neuroimage 145:24–43
14. Koch KM, Nencka AS, Klein A, et al. (2023) Diffusion-weighted MRI of the spinal cord in cervical spondylotic myelopathy after instrumented fusion. Frontiers in Neurology 14:1172833
15. Van Griethuysen JJ, Fedorov A, Parmar C, et al. (2017) Computational radiomics system to decode the radiographic phenotype. Cancer research 77:e104–e107
16. LeDell E, Poirier S (2020) H2O AutoML: Scalable automatic machine learning. 7th ICML Workshop on Automated Machine Learning (AutoML)